JOINT INSTITUTE FOR AERONAUTICS AND ACOUSTI

National Aeronautics and
Space Administration

Ames Research Center

Stanford University

JIAA TR-88

A TWO DIMENSIONAL STUDY OF ROTOR/AIRFOIL INTERACTION IN HOVER

By

CHYANG S. LEE

Stanford University
Department of Aeronautics and Astronautics

August 1988

ABSTRACT

This report documents a two dimensional model for the chordwise flow near the wing tip of the tilt rotor in hover. The airfoil is represented by vortex panels and the rotor is modeled by doublet panels. The rotor slipstream and the airfoil wake are simulated by free point vortices.

Calculations on a 20% thick elliptical airfoil under a uniform rotor inflow are performed. Variations on rotor size, spacing between the rotor and the airfoil, ground effect, and the influence upper surface blowing on download reduction are analyzed. Rotor size has only a minor influence on download when it is small. Increase of the rotor/airfoil spacing causes a gradual decrease on download. Proximity to the ground effectively reduces the download and makes the wake unsteady. The surface blowing changes the whole flow structure and significantly reduces the download within the assumption of a potential solution. Improvement on the present model is recommended to estimate the wall jets induced suction on the airfoil lower surface.

NOMENCLATURE

A_a	airfoil projection area
A_r	rotor disk area
c	airfoil chord
C_d	download coefficient
C_p	surface pressure coefficient
D	airfoil download
h	height of the airfoil above ground
$\triangle l$	panel length
p	static pressure
P	total pressure
R	rotor size
$\triangle s$	separation point displacement
t	time
T	rotor thrust
U, V	horizontal and vertical velocities
U_e	boundary edge velocity
V_r	rotor inflow
V_u	downwash velocity in far wake
x, y	horizontal and vertical coordinates
γ	vorticity, circulation per unit length
Γ	strength of wake vortex
Ψ	stream function

1. INTRODUCTION

Interactions between the rotors and wing of a tilt rotor aircraft in hover and low speed flight have a significant detrimental effect of its payload performance. The reduction of payload results from the impingement of the wake of lifting rotors on the wing, which is at -90° angle of attack in hover. The corresponding flow field involves bluff body separation from both leading and trailing edges of the wing, resulting in a large downward force. This vertical drag is often referred as the 'download' of a tilt rotor. The download penalty was estimated to be as much as 15% of the total thrust in hover.[1] Modifications on the wing, such as large deflected flaps, tangential blowing on leading and trailing edges, were suggested to improve the payload of the aircraft.[1,2,3]

The flow field in this problem is very complex, and includes unsteady, three-dimensional, rotational, separated flow and ground effect. Flow visualization has shown that the flow near the wing root region is mainly spanwise, and moving upwards on the symmetry plane, resulting in a fountain on each side of the airplane centerline. The flow near the wing tip is mainly chordwise, essentially a two-dimensional flow field [1], as shown in Fig. 1.

Accurate analysis of the download on tilt rotor configurations could provide the essential tool for designing an optimal wing to improve the hover performance. Most of the predictive methods reported in the literature are empirically deduced from experiments and restricted to the particular configuration.[3,4] For numerical predictions, Clark[5] used a steady panel method to calculate the wing/rotor interaction, but the emphasis was on the performance of the rotor in the presence of the wing, and no download datum was reported. McCroskey et. al.[6] calculated the two dimensional download problem in a uniform free stream. The rotor is not considered in their study, thus, the effect of rotor configuration and ground effect

was not investigated. No report can be found on theoretical studies on download reduction by upper surface blowing.

As a first step in understanding the effects of geometry parameters on the wing download, this report examines a simplified two-dimensional model to represent the chordwise flow near the wing tip. The rotor is simulated by doublet panels with known vertical velocity distribution, and a simple elliptical airfoil in the rotor wake is modeled by vortex panels. The shear layers generated by the rotor (tip vortices) and the separated wing wake are modeled by free point vortices in the flow field. The effect of surface blowing on download reduction is simulated by displacing the separation points on the wing lower surface. Parametric studies of the influence of download for varying rotor size, spacing between the rotor and the wing, in and out of ground effect, and displacement of separation points on the wing are presented in this report.

2. NUMERICAL IMPLEMENTATION

2.1 Simulation of the Airfoil and Separated Wake

The scheme employed in this study is the two-dimensional vortex tracing method. This method has been studied for decades and successfully applied to bluff bodies in low speed flow. The method is based on the vorticity transport equation with viscous terms neglected. The flow is assumed to be impulsively started at time zero. At each time step, the flow field is simulated by tracing the wake vortices and solving the associated potential flow problem. The limiting case of the time dependent calculation gives the steady state solution. Numerous references can be found on this topic. However, the calculation performed in this report is based on an early code developed for the airfoil-spoiler problem.[7] In addition to the standard two di-

mensional vortex tracing method, the code employs higher order vortex panels on the wing, point vortices with viscous cores in the wake, and merging of the far field wake vortices. The detailed description of the code development can be found in Ref. 7.

The separation points must be specified in the vortex method; this can be determined either from experimental evidence or a simple integral boundary layer analysis. For the download problem, however, the separation points are much easier to find, since they are fixed on the leading and trailing edges of the airfoil. When the upper surface blowing is applied, the separation points move toward the center of the airfoil along the lower surface. This can be easily modeled by displacing the separation points in the vortex method. More discussions on the blowing effect is presented in Section 3.4.

2.2 Simulation of the Rotor

A vortex panel produces a discontinuity in the tangential velocity along its surface in two-dimensional flows. For potential flow problems, vortex panels alone are sufficient to satisfy the flow tangency condition on the surface of a non-permeable body. On the rotor disk, however, the boundary condition is specified by a known normal velocity distribution. Therefore, doublet panels which induce velocities normal to their surfaces have to be employed. The expressions for the stream function and velocity induced by a doublet panel of unit strength centered at the origin, lying along the x-axis of the 'element coordinate system' can be derived as follows,

$$2\pi\Psi = \int \frac{(x-\xi)}{(x-\xi)^2+y^2} d\xi = -\frac{1}{2}\ln[\frac{(x-\frac{\Delta l}{2})^2+y^2}{(x+\frac{\Delta l}{2})^2+y^2}], \tag{1}$$

$$2\pi U = \int \frac{-2y(x-\xi)}{[(x-\xi)^2+y^2]^2} d\xi = -\frac{y}{(x-\frac{\Delta l}{2})^2+y^2} + \frac{y}{(x+\frac{\Delta l}{2})^2+y^2}, \tag{2}$$

$$2\pi V = \int \frac{(x-\xi)^2-y^2}{[(x-\xi)^2+y^2]^2} d\xi = \frac{x-\frac{\Delta l}{2}}{(x-\frac{\Delta l}{2})^2+y^2} - \frac{x+\frac{\Delta l}{2}}{(x+\frac{\Delta l}{2})^2+y^2}, \tag{3}$$

where Δl is the length of the doublet panel. The expression for the induced stream function is needed for satisfying the boundary condition of constant stream function along the wing surface, and the induced velocity is used for updating the position of wake vortices in the flow field.

2.3 Shedding of Rotor Vortices

The strength of wake vortex, Γ, shedding from a solid body is related to the strength of the bound vorticity (or the boundary layer edge velocity, U_e) at the separation point and the time step, Δt, as

$$\Gamma = \frac{1}{2} U_e^2 \Delta t. \tag{4}$$

This equation is derived from theoretical consideration and has been confirmed by many experimental studies.[7] For a thrust generating rotor, this relationship is no longer valid and a new expression has to be found.

The rotor energizes the flow field, and the total pressure below the rotor is higher than that of the surrounding fluid. The total pressure difference across the

stream tube downstream the rotor disk plane is manifested by free shear layers (slipstream) emanating from the edge of the rotor. Due to conservation of mass and momentum of the induced wake, the slipstream is always contracted as it moves downstream.

Assuming a uniform inflow of velocity V_r across the rotor disk, a simple momentum analysis[8] shows that for a hovering rotor, the relation between V_r and the 'ultimate velocity' in far downstream V_u, is

$$V_u = 2V_r. \tag{5}$$

The strength of the shear layers shed from the rotor tip, γ, is related to the difference in total pressure across the slipstream, ΔP, as

$$\Delta P = \rho V_r \gamma. \tag{6}$$

ΔP can be obtained by considering the total pressure variation along the center of the rotor disk as shown in Fig. 2. The total pressure in far upstream at $y = \infty$, just above the rotor at $y = 0^+$, just below the rotor at $y = 0^-$, and in the far wake at $y = -\infty$ are

$$
\begin{aligned}
P_\infty &= p_\infty, \\
P_{0+} &= P_\infty = p + \frac{1}{2}\rho V_r^2, \\
P_{0-} &= p + \frac{1}{2}\rho V_r^2 + \Delta P, \\
P_{-\infty} &= P_{0-} = p_\infty + \frac{1}{2}\rho V_u^2,
\end{aligned}
\tag{7}
$$

where p is the static pressure. Combining the above equations,

$$
\begin{aligned}
\Delta P = P_{0-} - P_{0+} &= \frac{1}{2}\rho(V_u^2 - V_r^2) = \frac{3}{2}\rho V_r^2, \\
\gamma &= \frac{3}{2}V_r.
\end{aligned}
\tag{8}
$$

Therefore, the strength of the shedding vortex from the rotor tip is

$$
\Gamma = \frac{3}{2}V_r^2 \Delta t, \tag{9}
$$

which is three times larger the similar expression for the wake shed from the wing in Eq. 4. Notice that this equation is derived from the assumption of constant velocity across the rotor disk. If the velocity distribution is not uniform, the ratio of V_u and V_r will not be 2, and the coefficient in Eq. 9 will also be different.

2.4 Normalization of Coefficients

The characteristic velocity for the download problem is the velocity across the rotor disk, V_r. For normalization of the surface pressure coefficient on the airfoil, a convenient choice is the dynamic pressure on the rotor disk,

$$C_p = \frac{p - p_\infty}{\frac{1}{2}\rho V_r^2}. \tag{10}$$

Since the airfoil is immersed in the high energy flow below the rotor, the total pressure in this region is

$$P = p + \frac{1}{2}\rho V^2 = p_\infty + \frac{1}{2}\rho V_u^2.$$

Rearranging this equation and substituting it into Eq. 10, the expression for pressure coefficient can be simplified as

$$C_p = 4 - (\frac{V}{V_r})^2. \tag{11}$$

Download coefficient is obtained by integrating C_p along the airfoil surface,

$$C_d = \oint C_p d(\frac{x}{c}), \tag{12}$$

and the download on the airfoil is

$$D = C_d \frac{1}{2} \rho V_r^2 A_a,$$

The rotor thrust equals to the total momentum flux in far downstream, therefore,

$$T = (\rho A_r V_r) V_u = 2\rho A_r V_r^2,$$

where A_a and A_r are the projection area of the airfoil and the rotor respectively. Combining these two equation, the ratio of download to thrust is

$$\frac{D}{T} = \frac{C_d}{2} \frac{A_a}{A_r}. \tag{13}$$

3. NUMERICAL RESULTS

Calculations were performed on a 20% thick elliptical airfoil below a rotor disk. Parametric studies of the download on the airfoil were made by varying rotor size R, spacing between the rotor and airfoil d, height above ground h, and displacement of separation points $\triangle s$. The parameters are varied from the typical dimension of the V-22 tilt rotor aircraft at wing tip, which are $R = 4.8$, and $d = 2.2$. The length is normalized by the airfoil chord.

The calculated streamline plot of a typical case of $R = 4.5$ and $d = 2.5$ is shown in Fig. 3. The contraction of the rotor slipstream is shown clearly by the streamlines. The point vortices are represented by circles and crosses, corresponding

to the clockwise and counter-clockwise vortices respectively. The size of the vortices is proportional to their strength. The vortices shed from the rotor and the airfoil are rotating in different directions, indicating that the slipstream from the rotor adds energy into the flow, while the shear layers from the airfoil takes kinetic energy away from the wake. The shear layers shed from both sides the airfoil are about the same strength by examining the sizes of the vortices. However, the sizes of vortices from the rotor tips are less uniform and are distributed over a wider area along the slipstream. This is the result of both the vortex interactions and the merging of rotor vortices. Although the wake vortices from the airfoil are also subject to merging, the merging is made to take place far downstream in the calculation, since a reasonable resolution near the airfoil is required to obtain a good download estimation. The other possible explanation for the randomness of the rotor vortices is the fact that the rotor tip vortex in three-dimensional flow is unstable, and the present 2-D calculation could accidentally reproduce the instability of the real flow.

The pressure distribution of the same configuration is presented in Fig. 4. This is similar to the usual two-dimensional symmetrical bluff body in a free stream except that the scale of the present calculation is much larger. The value of C_p at the stagnation point on the airfoil upper surface is 4 instead of the usual value 1 for surfaces in free stream. The reason is that pressures are normalized by the dynamic pressure at the rotor disk. If the reference plane is chosen at $y = -\infty$, and V_u is used for normalization, a stagnation pressure coefficient of 1 can be obtained. The constant pressure on the lower surface is typical for bluff body flow, and often referred as 'base pressure'.

3.1 Effect of Rotor Size

The effect of rotor diameter is shown in Figs. 5. The symbols are calculated

results and the line is the best fit curve. The download coefficient increases with rotor diameter, and levels off quickly when R is larger than 4 as shown in Fig. 5-a. Since the inflow velocity is fixed in the calculation, thrust is proportional to the rotor size. Therefore, the ratio of download to thrust decreases with R as shown in Fig. 5-b.

The change of download coefficient with rotor size can be examined further by comparing the pressure distribution for $R = 2.0$ and $R = 4.5$ as shown in Fig. 6. Pressure coefficients are identical in the base flow region on the lower surface for these two cases, therefore, the increase of download comes from the reduced suction on the upper surface as the rotor diameter increases. This effect is clearly illustrated in the flow field plot for the small rotor in Fig. 7. Compared with Fig. 3, this figure shows a narrower spacing between streamlines, indicating higher velocities in the flow. Larger suction is therefore induced on the upper surface, thereby reducing the download. The base pressure region does not change with the flow field velocities, since it is inside the 'dead water' of the base flow. As the rotor diameter increases, this 'edge effect' on the wing becomes less important, and the download slope approaches zero.

3.2 Effect of Rotor/Airfoil Spacing

The variation of download with spacing between the rotor and the airfoil is shown in Fig. 8. As expected, the download decreases as the spacing increases, since the interference between the rotor and wing tends to decrease as they are further apart. This effect can also be observed by the streamline plot shown in Fig. 9, which shows larger streamline deflection near the airfoil than that shown in Fig. 3.

The pressure distribution for the small spacing ($d = 0.5$) is plotted in Fig. 10;

also shown in the figure is the reference case of $d = 2.0$ for comparison. The pressures on both the upper and lower surfaces decrease with the rotor/airfoil spacing. This is due to the fact that the low pressure on the upper surface is induced by the high flow field velocity, and this effect is larger when the rotor and the airfoil is closer. The strength of the separated shear layer also increases with the decreasing rotor/airfoil spacing, thereby producing larger suction in the base pressure region. However, the increased suction on the upper surface is less pronounced than the reduced base pressure on the lower surface; therefore, the integrated downward force increases with the spacing.

3.3 Ground Effect

The ground effect is simulated by including a mirror image system below the ground plane in the calculation. The download variation with the height above ground (measured from the airfoil position) is presented in Fig. 11. The dash line is the asymptotic value for out of ground effect. The download decreases rapidly with the height above ground, and the data deviate from the best fit curve as h decreases. This scatter is due to unsteadiness in the calculated results. Calculation shows that the airfoil wake becomes unstable as it is moving closer to the ground. The unstable wake can induce large loading fluctuations as the airfoil is also close to the ground. This phenomenon is clearly demonstrated in the streamline plot of $h = 3.0$, as shown in Fig. 12. A large ground vortex is formed by the left side of the airfoil wake, resulting in an asymmetrical flow field. A concentrated counter-rotating wake is also forming from the right side of the airfoil and being washed downwards. The alternating wake vortices are similar to Karman vortices in the free stream flow. These fluctuating loads on the airfoil might cause control problem during take off and landing.

Fig. 13 compares the pressure distribution on the airfoil with and without ground effect. The decrease of download with the ground effect results from the reduced suction in the base pressure region, and the pressure on the upper surface is about the same. This suggest that the proximity of ground only has a local effect on the airfoil lower surface.

3.4 Effect of Separation Point Displacement

The effect of tangential blowing on the upper surface is simulated by separation point displacement. Symmetrical blowing is assumed, i.e. the displacement of separation points is the same on both leading and trailing edges. Variation of separation point displacement with download is presented in Figs. 14., where Δs represents the distance between the separation point and the edge. To illustrate the effectiveness of download reduction, the download coefficient is normalized by C_d with no separation point displacement. The plot shows a large negative slope with small separation point displacement, and reaches an asymptotic value of 75% download reduction when the separation points are moved 20% from the edges.

The salient change of the wake characteristics due to separation point displacement is illustrated in Figs. 15. The dramatic effect of 1% separation displacement on the flow field is shown in Fig. 15-a. Comparing with Fig. 3, the wake contracts if separation points are moved only 1% from the edges, whereas the wake diverges when no separation control is applied. At 10% displacement, the wake is closed as shown in Fig. 15-b. Examining the streamline patterns above and below the airfoil for 10% displacement, the rotor wake almost recovers its original shape without the airfoil. Therefore, a large reduction in download on the airfoil can be expected.

Fig. 16 illustrates the change in pressure distribution due to the separation point displacement. Comparing with the case for natural separation, the pressure

changes on both upper and lower surfaces. However, the major contribution to the download reduction comes from the reduced pressure on the upper surface, while little change is observed in the base pressure region on the lower surface. This is consistent with the experimental observations reported in Ref. 3. The explanation is following: The flow accelerates due to the the large surface curvature near the edges when the flow is attached, inducing considerable suction on the upper surface as the flow is trying to turn around and remain attached on the airfoil lower surface. For natural separation, however, the flow leaves the airfoil smoothly into the wake at the edges. This requires less acceleration since the streamline curvature is much less than the surface curvature of the airfoil; therefore, the corresponding suction generated on the upper surface is less than that of the attached flow. The base pressure depends on the strength of the separated shear layer. In the present configuration, the change in wake strength with separation point displacement is relatively small, which can be verified by comparing the size of the airfoil wake in Figs. 3 and 16. Therefore, the base pressure is almost the same for both cases.

In simulation of surface blowing by the present potential method, the viscous effect of energizing the boundary layer near the natural separation point is neglected. Wall jets on a curved surface produce pressure gradients in the normal direction to balance the centrifugal force required to turn the flow inside the jet layer. This pressure gradient induces suction on the surface. The magnitude of this suction depends on the jet velocity and the surface curvature. When the wall jet is used to displace separation, the jet is generally placed just upstream of the natural separation points. The surface curvature is usually large near the separation points, thereby inducing large suction along the surface till the flow is separated. This effect may produce considerable suction on the airfoil lower surface, thereby decreasing the effectiveness of surface blowing on download reduction. Though it is important, the term is not considered in the present calculation. Integral methods can be

coupled with the present analysis to give a more realistic estimation of effect of upper surface blowing. With some modifications to account for the outer potential flow solution, the analytical model for the curved wall jets in quiescent flow reported in Ref. 9 should be a good start for improvement of this aspect of the problem.

4. CONCLUDING REMARKS

A simple two dimensional scheme has been developed to model the chordwise flow near the wing tip for the download problem. The effects for rotor size, spacing between the rotor and the wing, ground effect, and the separation point displacement are investigated for a 20% elliptical airfoil under a uniform rotor inflow.

Small rotors have larger download coefficients, but the effect diminishes when the rotor is larger than 4 times the airfoil chord. Download decreases with rotor/airfoil spacing. The increased download for small spacing is mainly due to the reduced base pressure on the airfoil lower surface.

Ground effect reduces the download. An unstable, alternating wake makes the download unsteady when the airfoil is very close to ground. The proximity of ground has only a local effect on the airfoil lower surface, while the upper surface pressure is not changed.

The effect of tangential upper surface blowing is modeled by displacing the separation points from their original location. A small displacement of the separation points on the airfoil can completely change the whole flow field structure. The download reduction is most effective at small separation point displacements. At 10% separation point displacement on both sides of the airfoil, the wake is almost closed and the flow around the airfoil recovers its potential solution. The download reduction mainly comes from the reduced pressure on the airfoil upper surface, with

little change in the base pressure. Integral methods are suggested to estimate the additional low pressure on the airfoil lower surface due to the viscous effect of curved wall jets, which are not considered in this report but might significantly degrade the effectiveness of the upper surface blowing.

6. REFERENCE

1. Felker, F. F. and Light, J. S., "Aerodynamic Interactions Between a Rotor and Wing in Hover", Journal of the American Helicopter Society, Vol. 33, No. 2, pp. 53-61, April 1988.

2. Felker, F. F., Signor, D. B., Young L. A., and Betzina, M. D., "Performance and Loads Data From a Hover Test of a 0.658-Scale V-22 Rotor and Wing", NASA TM-89419, April 1987.

3. Faye, R. E., Felker, F. F. and Light, J. S., "An Assessment of Upper Surface Blowing for the Reduction of Tilt Rotor Download", AIAA 5th Applied Aerodynamics Conference, 1987.

4. McVeigh, M. A., "The V-22 Tilt-Rotor Large-Scale Rotor Performance/ Wing Download Test and Comparison with Theory", 11th European Rotorcraft Forum, 1985.

5. Clark, D. A., "Analysis of the Wing/Rotor And Rotor/Rotor Interactions Present in Tilt-Rotor Aircraft", Vertica, Vol. 11, No. 4, pp. 731-749, 1987.

6. McCroskey, W. J., Spalart, P., Laub, G. H., Maisel, M. D., and Maskew, B., "Airloads on Bluff Bodies, With Application to the Rotor-Induced Downloads on Tilt-Rotor Aircraft", Vertica, Vol. 9, No. 1, pp 1-11, 1985.

7. Lee, C. S., and Bodapati, S., "Calculation of the Unsteady Flow Field of an Airfoil with a Deflected Spoiler by Vortex Method", JIAA TR-62, Department of Aeronautics and Astronautics, Stanford University, 1985.

8. W. Z. Stepniewski, "Rotorary Wing Aerodynamics", Dover Books.

9. Roberts, L., "A Theory for Turbulent Curved Wall Jets", AIAA paper 87-0004, 1987.

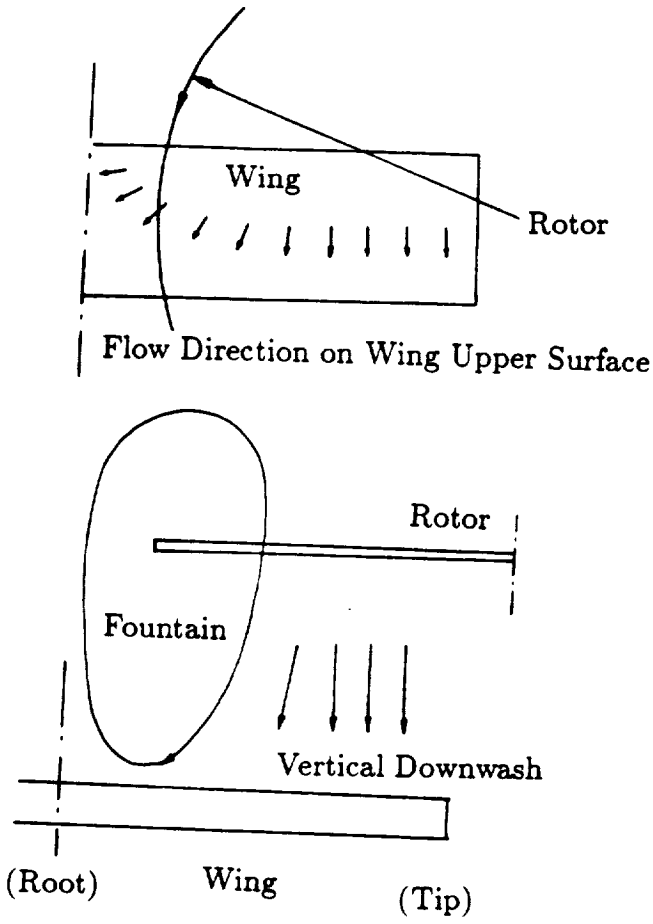

Fig. 1. Flow Filed of a Tilt Rotor in Hover.

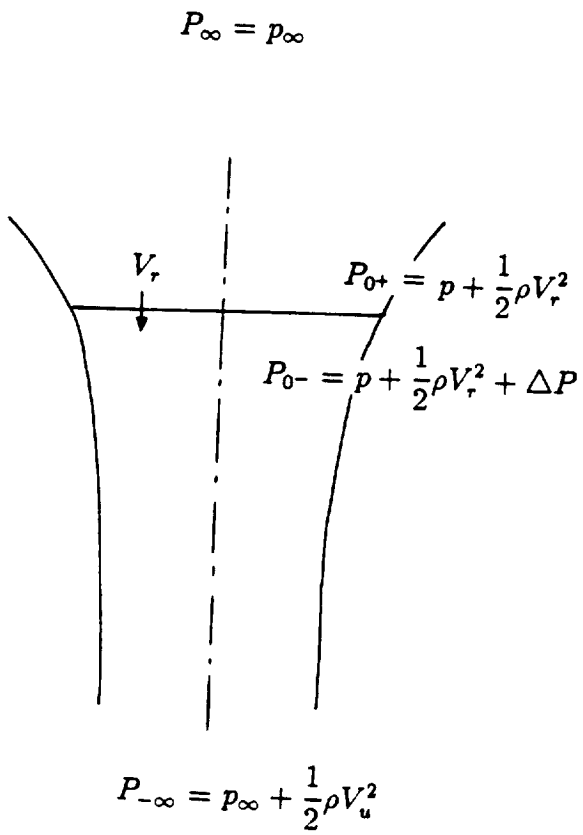

Fig. 2. Total Pressure Variation of a Hovering Rotor.

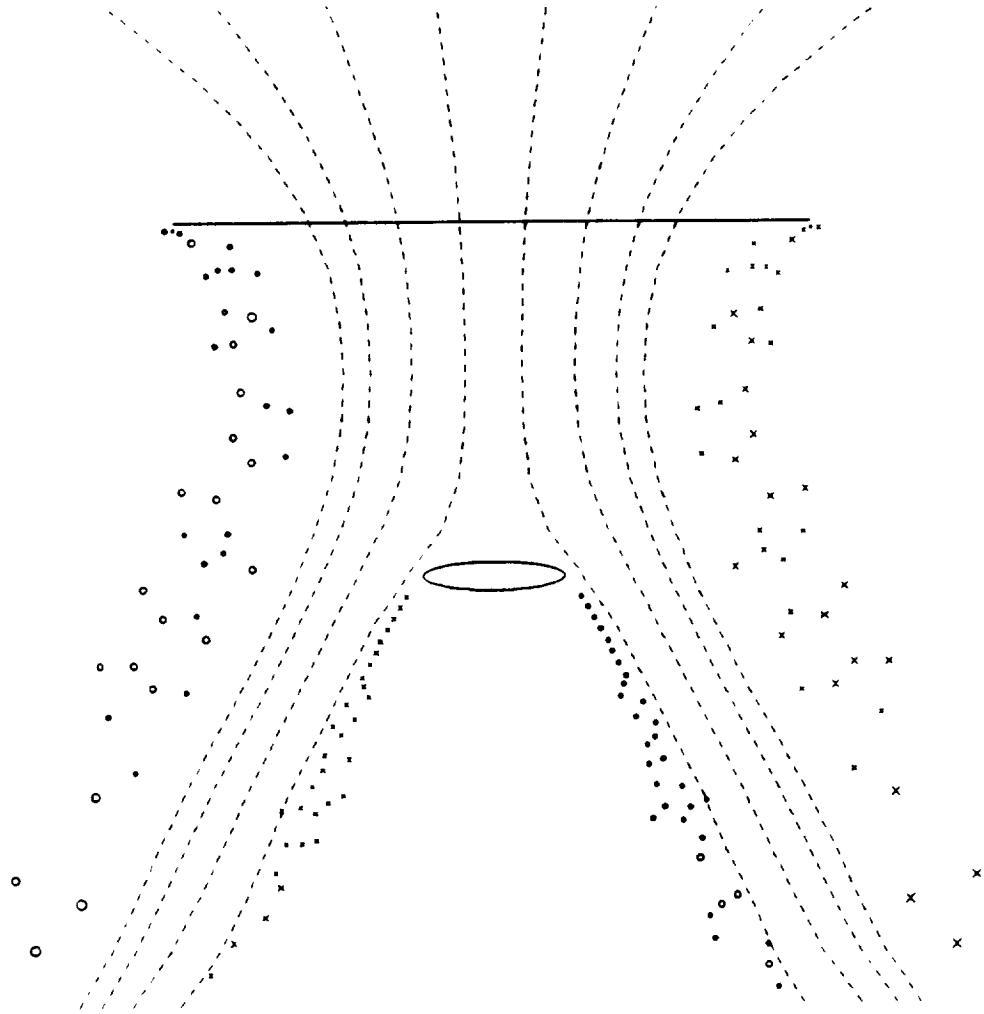

Fig. 3. Flow Field of a Typical Rotor/Airfoil Configuration. ($R = 4.5, d = 2.5$)

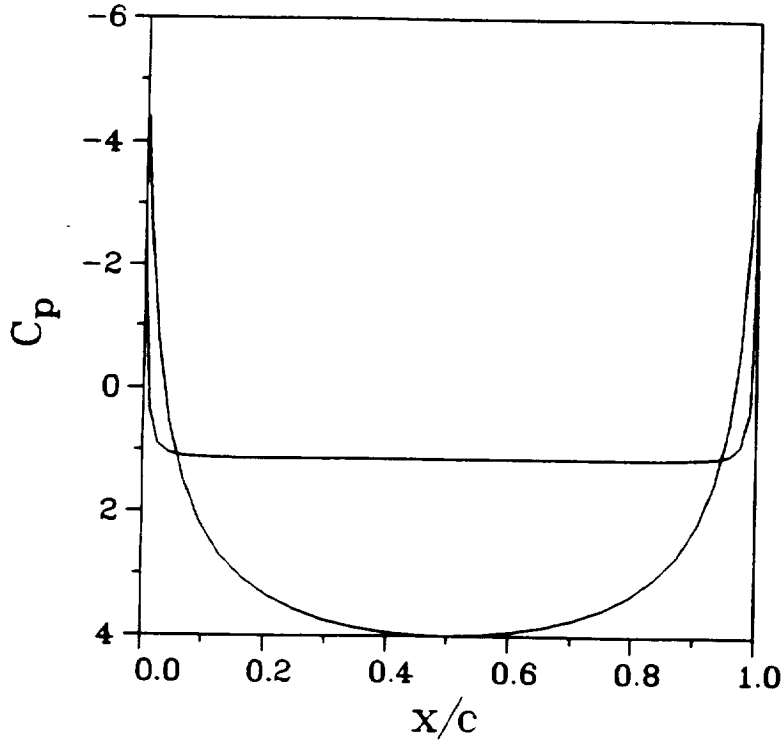

Fig. 4. Typical Airfoil Surface Pressure Distribution. ($R = 4.5, d = 2.5$)

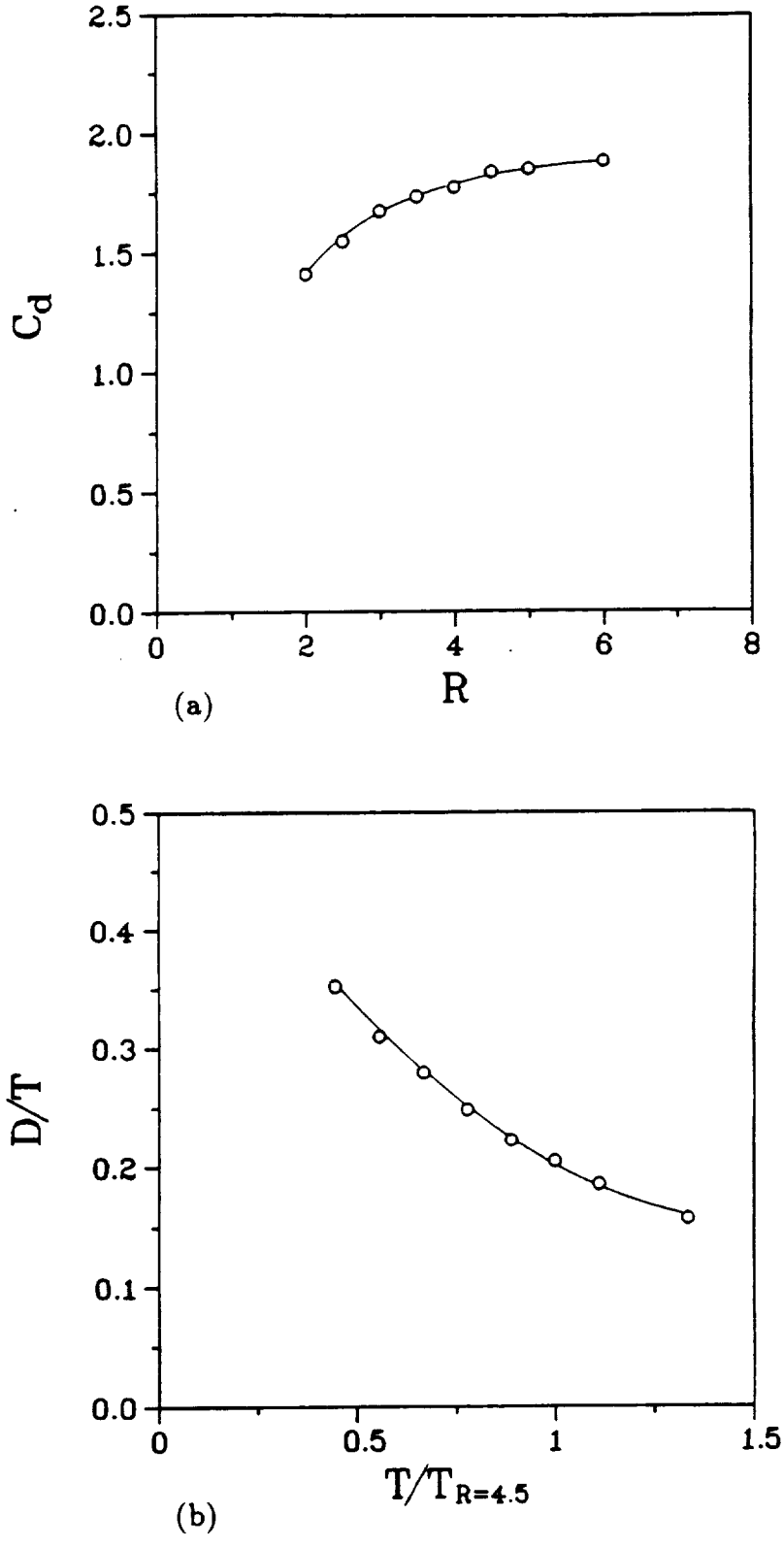

Fig. 5. Download Variation with Rotor Size.

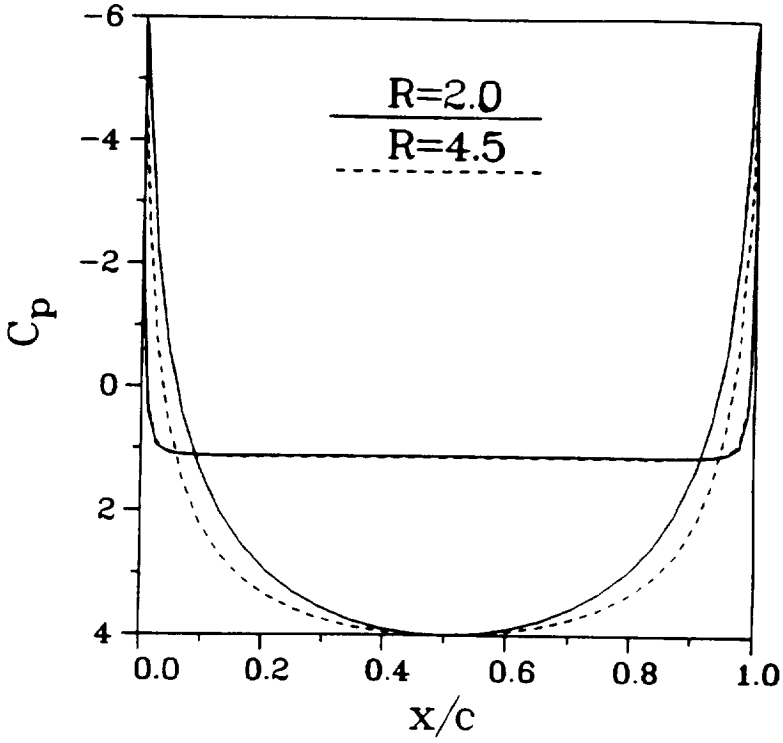

Fig. 6. Effect of Rotor Size on Airfoil Surface Pressure Distribution.

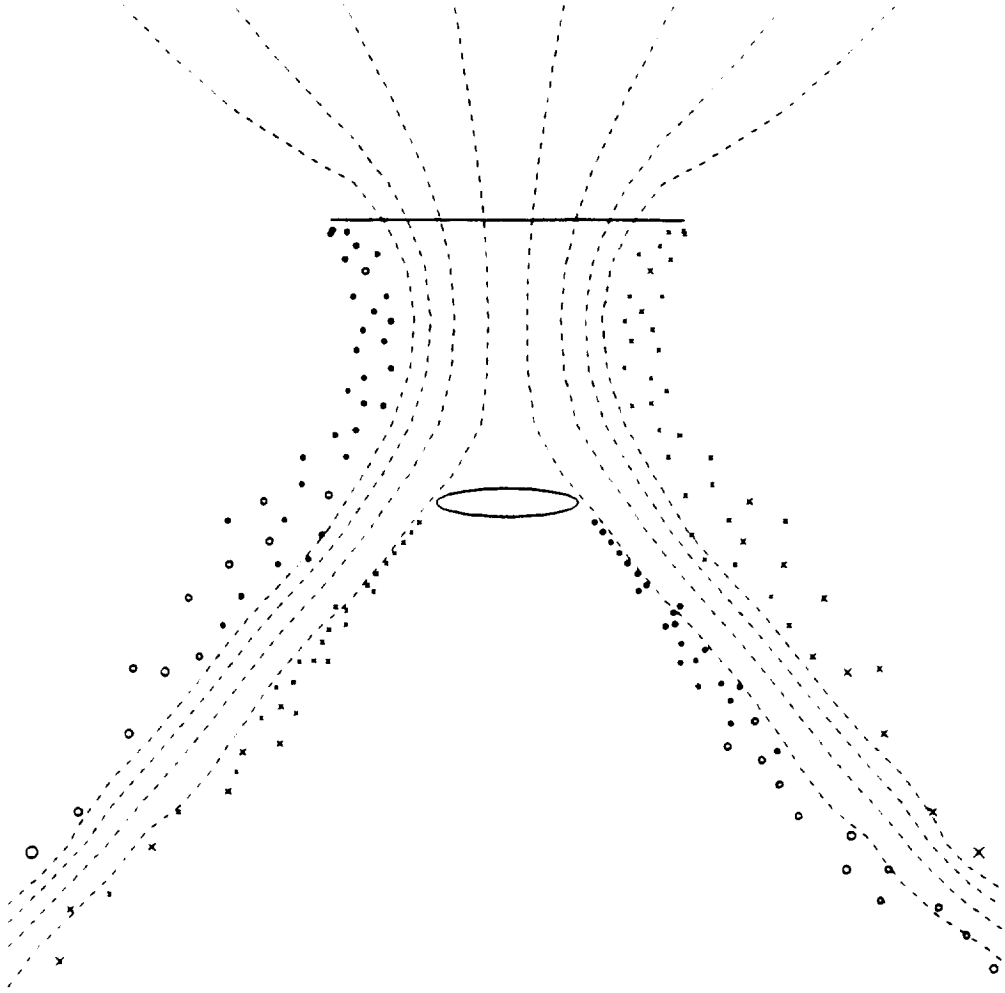

Fig. 7. Flow Field of the Download Problem with a Small Rotor. ($R = 2.0, d = 2.0$)

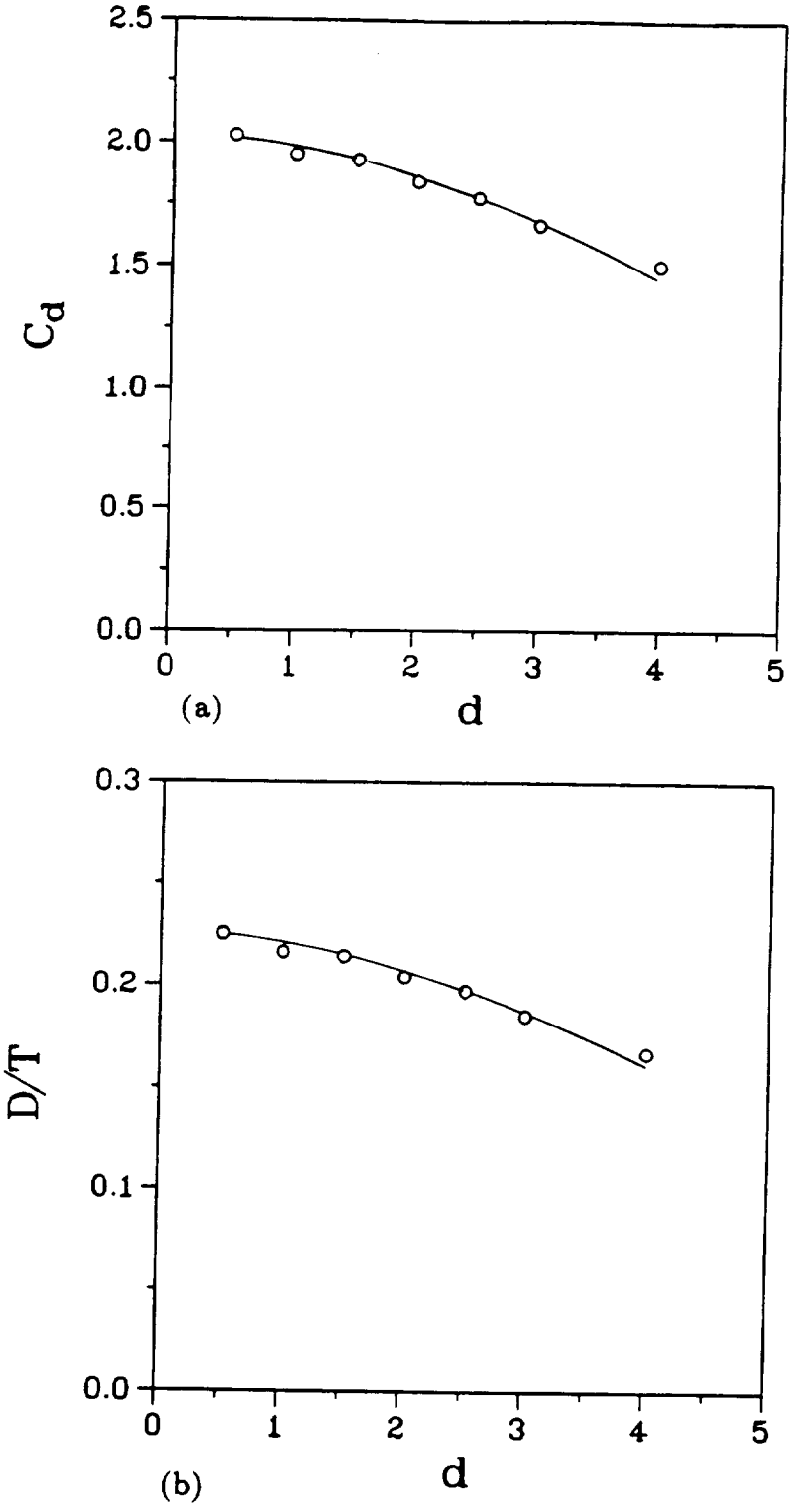

Fig. 8. Download Variation with Rotor/Airfoil Spacing.

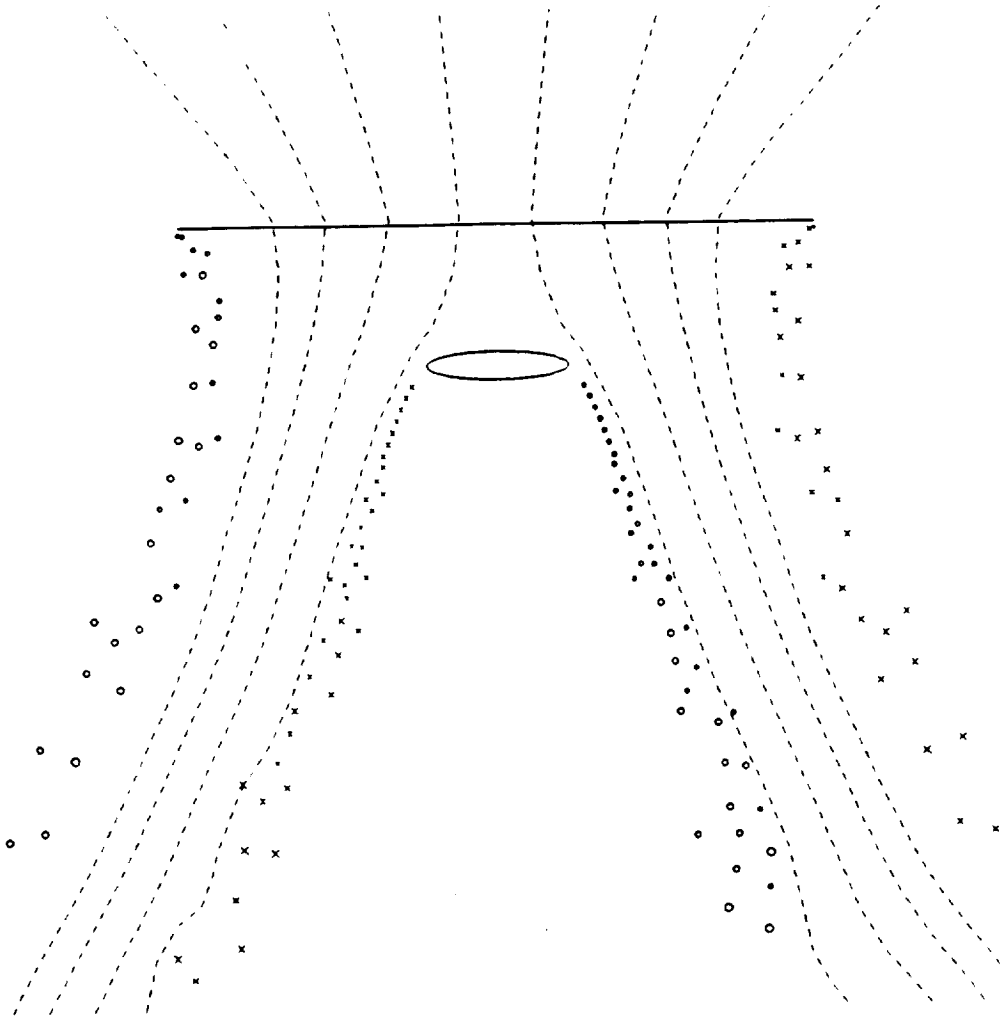

Fig. 9. Flow Field of the Download Problem with a small Rotor/Airfoil Spacing.

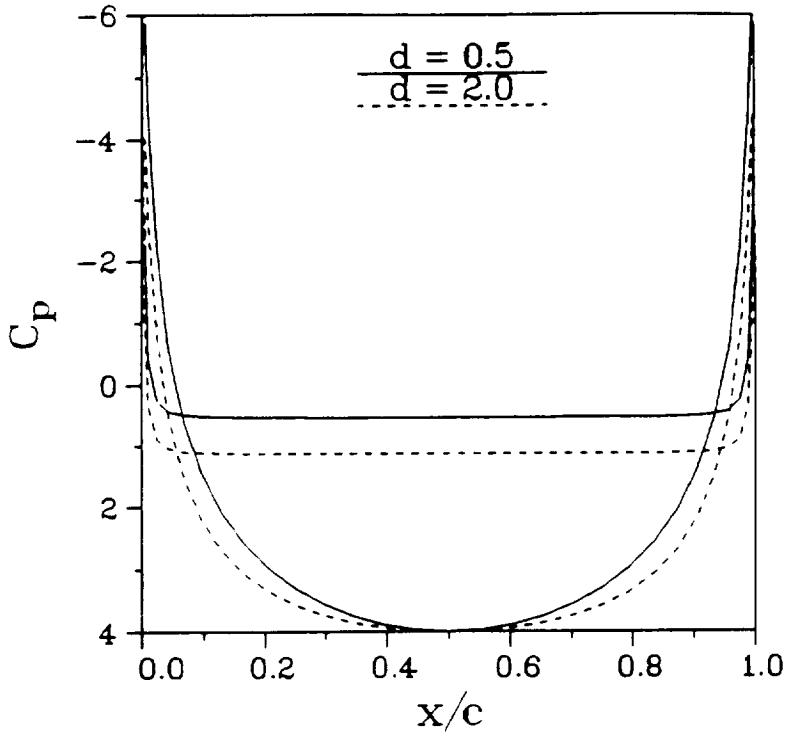

Fig. 10. Effect of Rotor/Airfoil Spacing on Airfoil Surface Pressure Distribution.

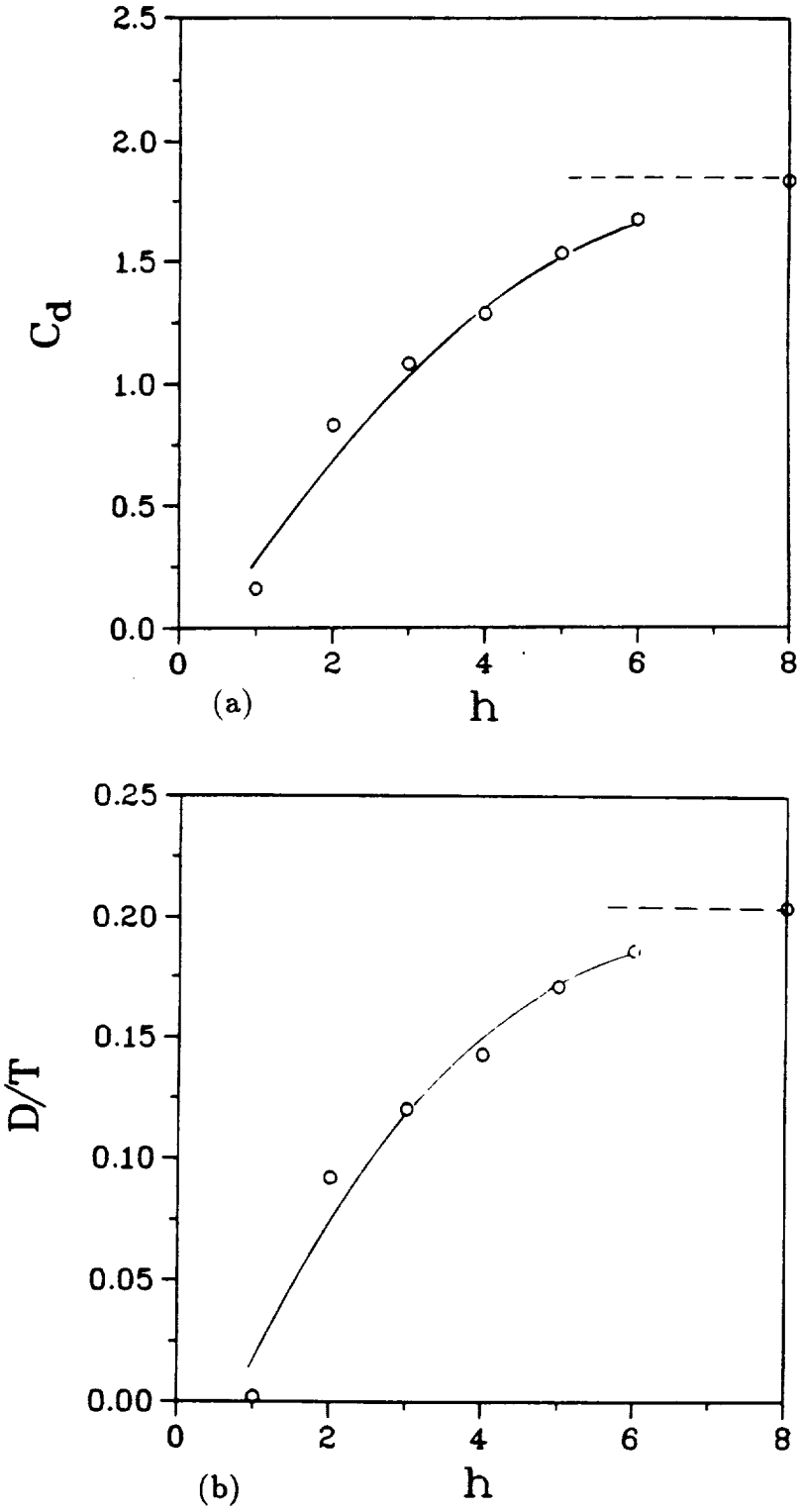

Fig. 11. Download Ground Effect.

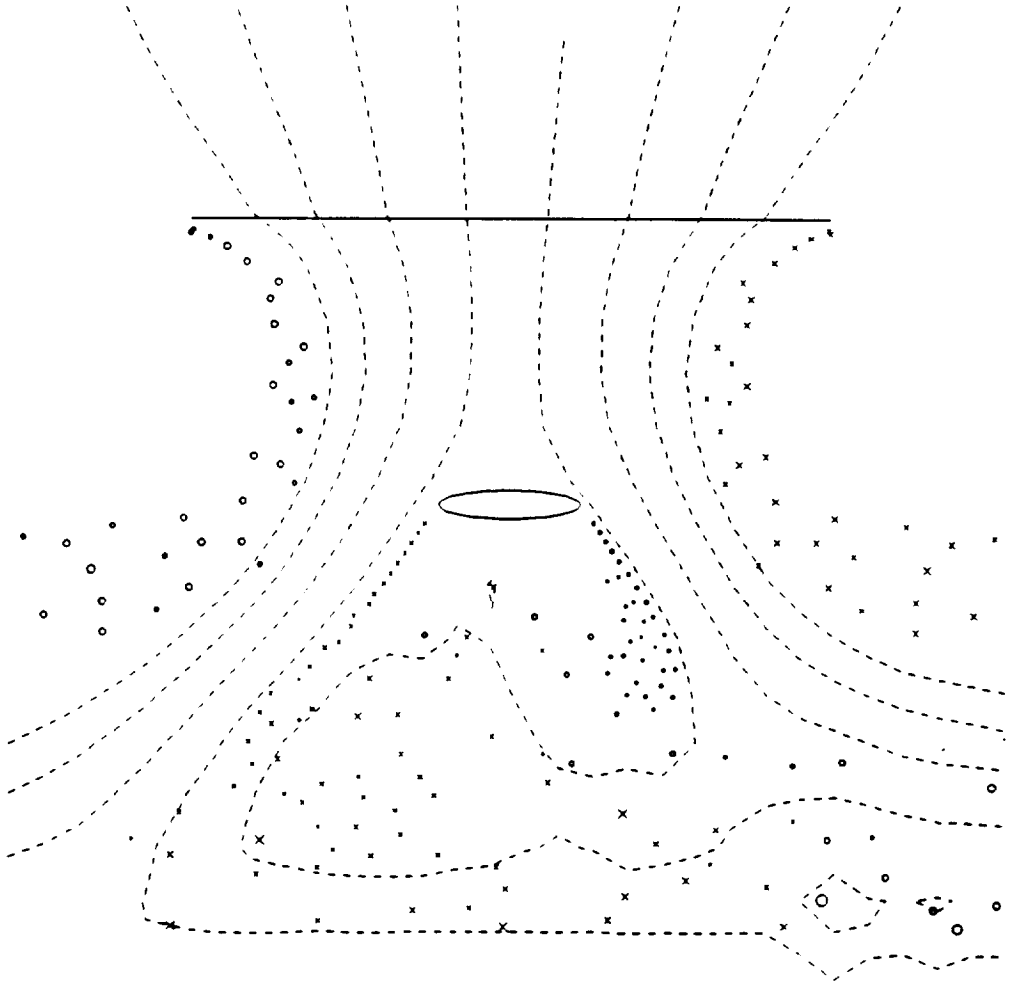

Fig. 12. Asymmetrical Wing Wake in Ground Effect.

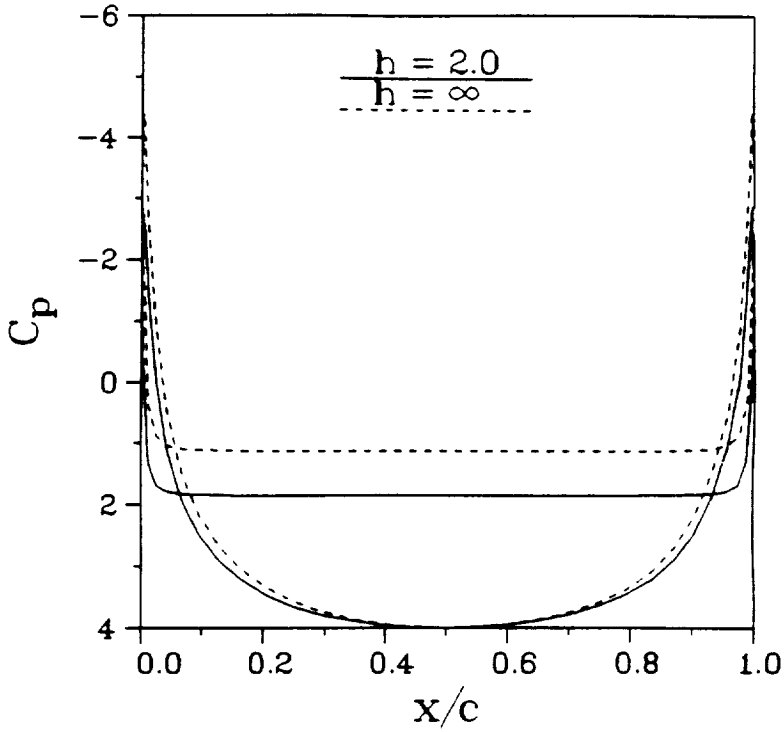

Fig. 13. Ground Effect on Airfoil Surface Distribution.

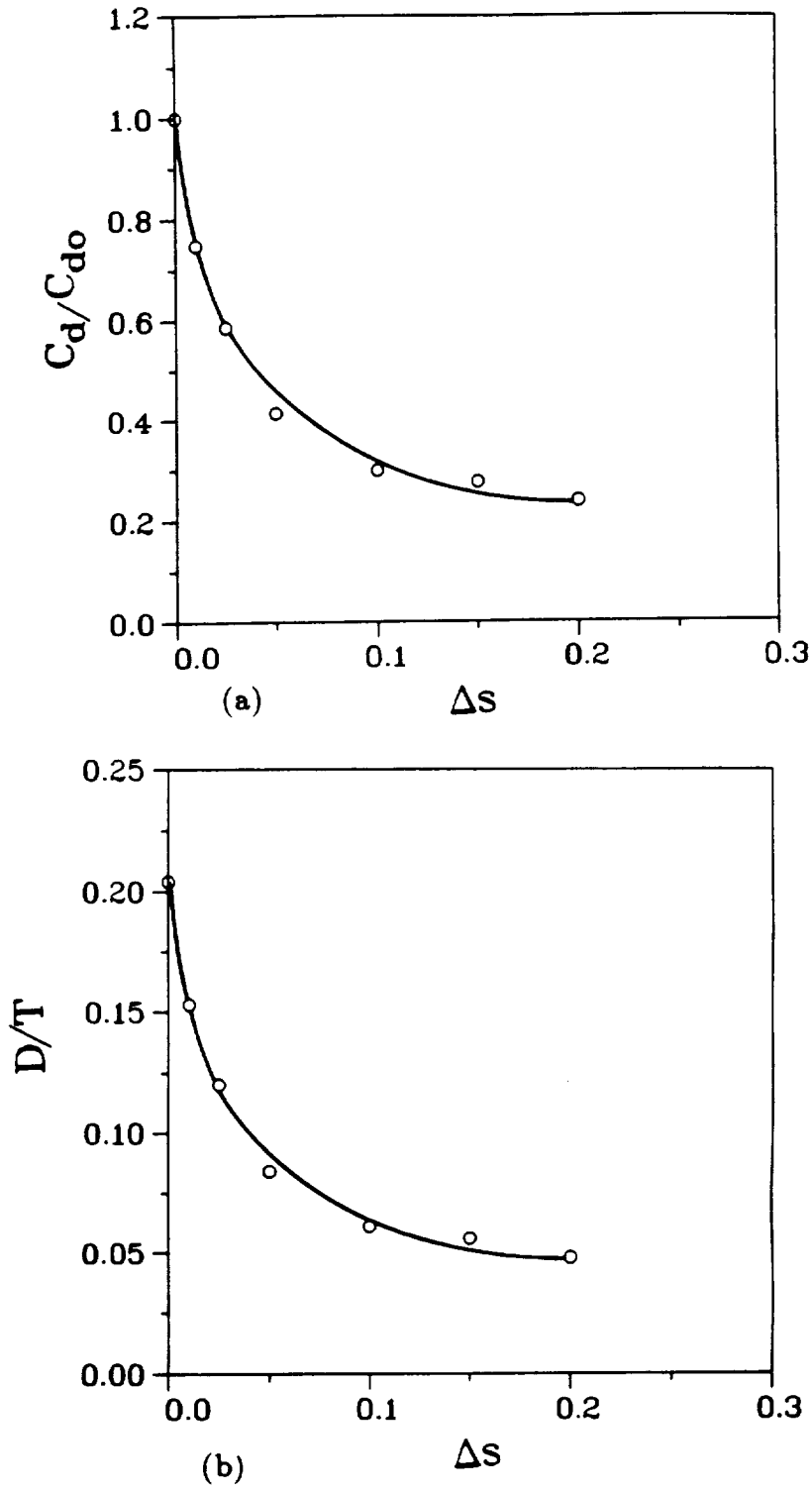

Fig. 14. Download Variation with Displacement of Separation Point.

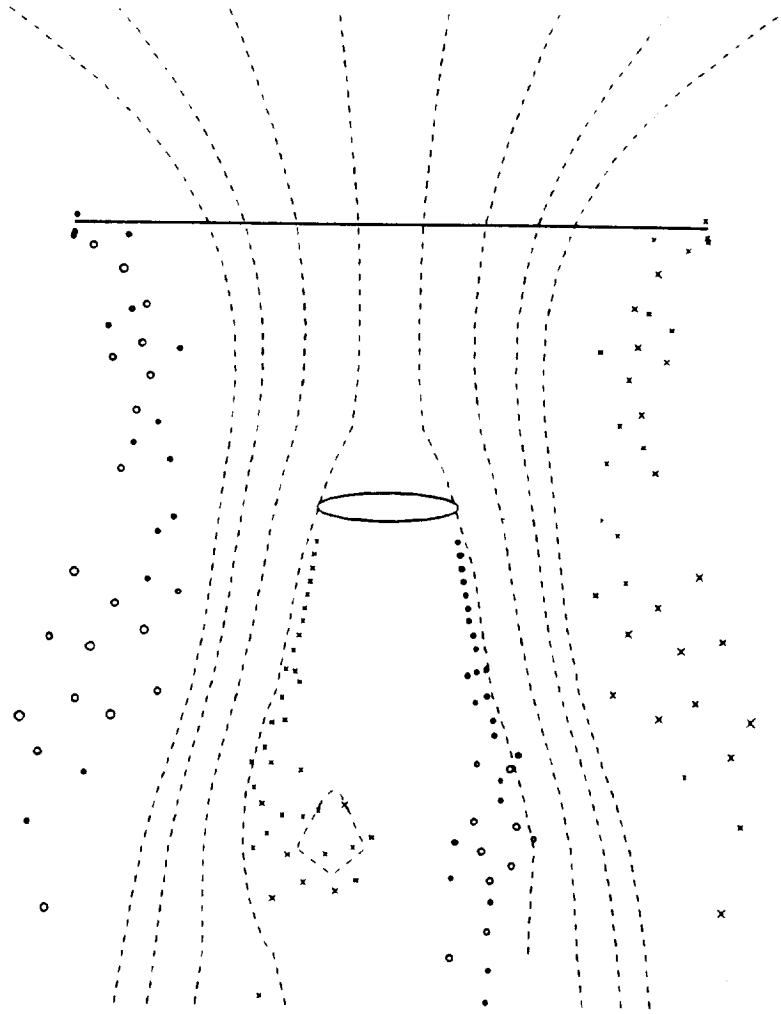

(a) $\Delta s = 0.01, R = 4.5, d = 2.0$

Fig. 15. Effect of Separation Point Displacement on the Flow Field.

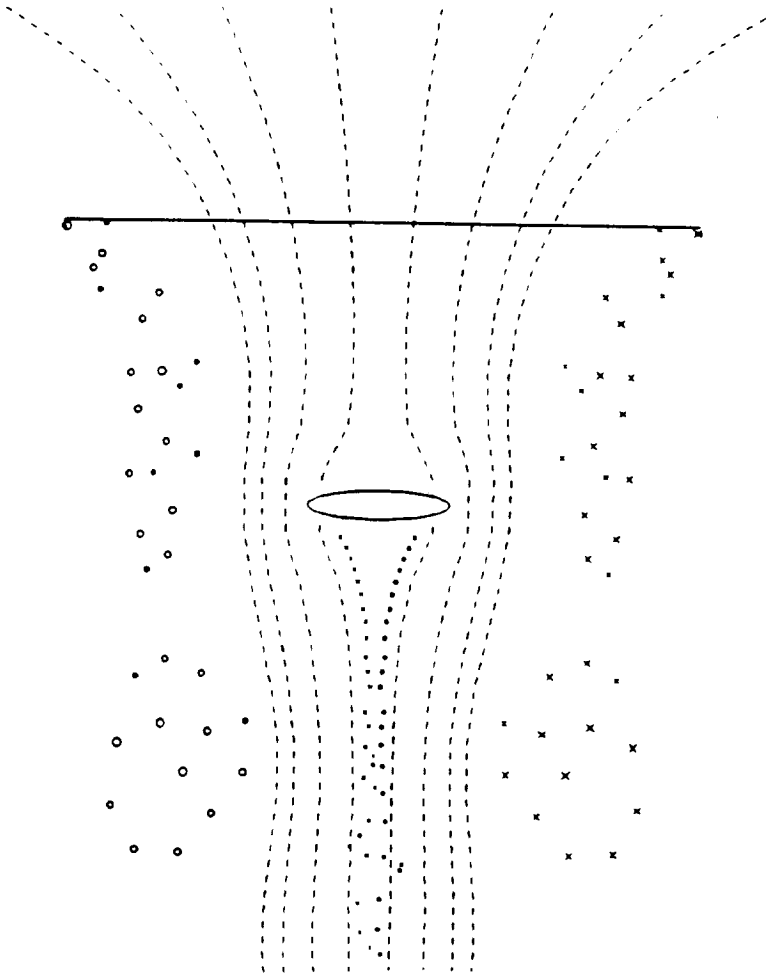

(b) $\Delta s = 0.10, R = 4.5, d = 2.0$

Fig. 15. Effect of Separation Point Displacement on the Flow Field.

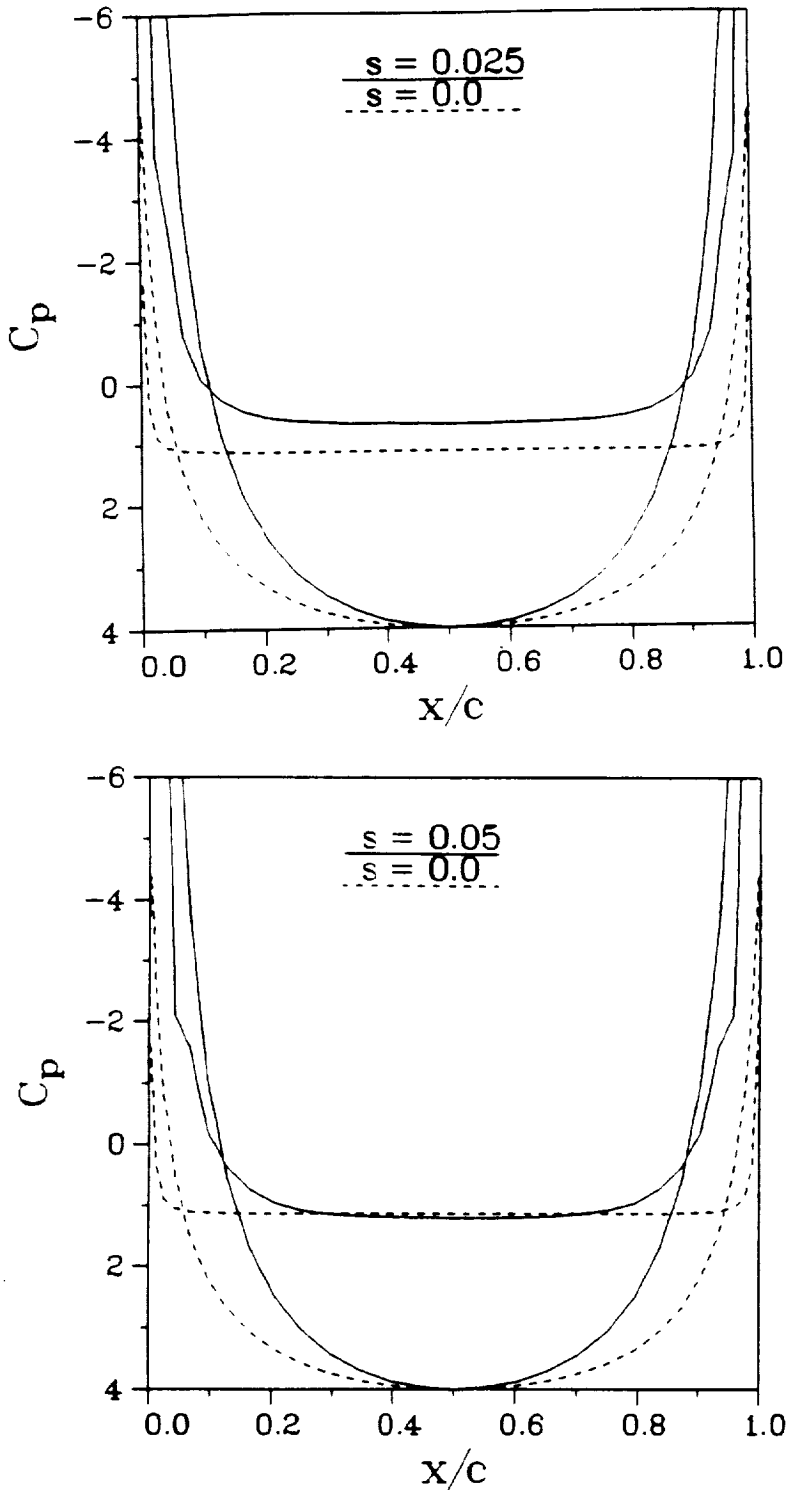

Fig. 16. Effect of Separation Point Displacement on Airfoil Surface Pressure